

Highly Strained, Ring-Tilted [1]Ferrocenophanes Containing Group 16 Elements in the Bridge: Synthesis, Structures, and Ring-Opening Oligomerization and Polymerization of [1]Thia- and [1]Senaferrocenophanes

Ron Rulkens, Derek P. Gates, David Balaishtis, John K. Pudelski, Douglas F. McIntosh, Alan J. Lough, and Ian Manners*

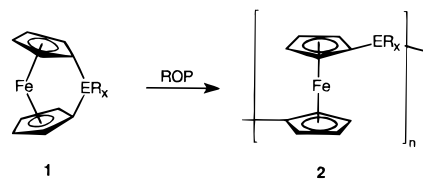
Contribution from the Department of Chemistry, University of Toronto, 80 St. George Street, Toronto, Ontario, M5S 3H6, Canada

Received June 20, 1997[⊗]

Abstract: The first chalcogen-bridged [1]ferrocenophanes $\text{Fe}(\eta\text{-C}_5\text{H}_3\text{R})_2\text{E}$ (**6**, E = S, R = H; **7**, E = Se, R = H; **12**, E = S, R = Me) have been synthesized and characterized both structurally and spectroscopically. Synthesis of sulfur- and selenium-bridged species **6** and **7** was achieved by the reaction of dilithioferrocene·TMEDA (TMEDA = tetramethylethylenediamine) with bis(phenylsulfonyl) sulfide $\text{S}(\text{O}_2\text{SPh})_2$ and selenium diethyldithiocarbamate $\text{Se}(\text{S}_2\text{CNEt}_2)_2$, respectively, in 20–30% yields. Structural characterization of both **6** and **7** revealed highly strained structures with tilt-angles between the cyclopentadienyl ligands of $31.05(10)^\circ$ and $26.4(2)^\circ$, respectively. Compounds **6** and **7** are purple and red-purple, respectively; comparison of the structures of known [1]ferrocenophanes **1** showed that when the second period (from group 14–16) is traversed, there is a substantial increase in cyclopentadienyl ring-tilting in main group element bridged [1]ferrocenophanes, and the lowest energy UV/vis absorption peaks become increasingly red-shifted. Extended Hückel MO calculations were performed and, consistent with this observation, predicted a decrease in the HOMO–LUMO gap as the ring-tilt increases. Thermal ring-opening polymerization (ROP) of both **6** and **7** afforded the insoluble poly(ferrocenyl sulfide) $[\text{Fe}(\eta\text{-C}_5\text{H}_4)_2\text{S}]_n$ **8** and poly(ferrocenyl selenide) $[\text{Fe}(\eta\text{-C}_5\text{H}_4)_2\text{Se}]_n$ **9**, respectively. Differential scanning calorimetry studies of the ROP process provided estimates of the strain energies of **6** and **7** which were ca. $130(\pm 20)$ and $110(\pm 20)$ kJ mol⁻¹, respectively. Anionic ROP of **6** also yielded the insoluble poly(ferrocenyl sulfide) **8**. However, linear soluble dimeric and trimeric trimethylsilyl-capped oligo(ferrocenyl sulfides) **10b** and **11b** were synthesized by the reaction of **6** with dilithioferrocene·TMEDA followed by the addition of Me_3SiCl and were characterized spectroscopically, electrochemically, and, for **11b**, by X-ray diffraction, and provide useful models for the analogous high polymer. The dimethylated sulfur-bridged species **12** was prepared as a mixture of isomers from the reaction between dilithiodimethylferrocene·TMEDA and $\text{S}(\text{O}_2\text{SPh})_2$, and X-ray structural characterization of a single isomer **12a** showed the presence of a large tilt-angle of $31.46(8)^\circ$. Thermal and anionic ROP of the isomer mixture **12** afforded the first soluble poly(ferrocenyl sulfide) $[\text{Fe}(\eta\text{-C}_5\text{H}_3\text{Me})_2\text{S}]_n$ **13** which was characterized by ¹H and ¹³C NMR, elemental analysis, thermogravimetric analysis, and gel permeation chromatography. Cyclic voltammetric studies of **13** showed the presence of two reversible oxidation waves with a redox coupling $\Delta E = \text{ca. } 0.32$ V, which is consistent with the presence of significantly stronger M···M interactions compared to those present in other ring-opened poly(ferrocenes) derived from [1]ferrocenophanes.

Introduction

Although the concept of bridging the cyclopentadienyl ligands of ferrocene with a single atom was at first dismissed since it was predicted that the resulting species would be too strained to exist,¹ the isolation of the first silicon-bridged [1]ferrocenophane **1** ($\text{ER}_x = \text{SiPh}_2$) in 1975 by Osborne and co-workers revealed that the ferrocene moiety is capable of supporting a surprising degree of strain.² X-ray structural studies of **1** ($\text{ER}_x = \text{SiR}_2$) and analogous species have revealed the presence of tilted cyclopentadienyl (Cp) ligands (interplanar tilt-angle (α) = $16\text{--}21^\circ$) as well as dramatic distortion at the *ipso*-carbon atoms where the angle between the Cp ligands and the *ipso*-carbon–silicon bond is $37\text{--}40^\circ$.^{3–6} Strained silicon-bridged [1]ferrocenophanes first attracted attention in the late 1970s as



surface derivitization agents,⁷ but more recently interest has been generated by the discovery that these species function as efficient precursors to high molecular weight poly(ferrocenylsilanes) **2** ($\text{ER}_x = \text{SiR}_2$) via thermal,⁸ anionic,^{9,10} or transition-metal-catalyzed^{11–13} ring-opening polymerization (ROP) reactions.

(4) Osborne, A. G.; Whiteley, R. H.; Meads, R. E. *J. Organomet. Chem.* **1980**, *193*, 345.

(5) Finckh, W.; Tang, B.-Z.; Foucher, D. A.; Zamble, D. B.; Ziembinski, R.; Lough, A.; Manners, I. *Organometallics* **1993**, *12*, 823.

(6) Pudelski, J. K.; Foucher, D. A.; Honeyman, C. H.; Lough, A. J.; Manners, I.; Barlow, S.; O'Hare, D. *Organometallics* **1995**, *14*, 2470.

(7) Fischer, A. B.; Kinney, J. B.; Staley, R. H.; Wrighton, M. S. *J. Am. Chem. Soc.* **1979**, *101*, 6501.

(8) Foucher, D. A.; Tang, B.-Z.; Manners, I. *J. Am. Chem. Soc.* **1992**, *114*, 6246.

[⊗] Abstract published in *Advance ACS Abstracts*, October 15, 1997.

(1) Neuse, E. W.; Rosenberg, H. J. *J. Macromol. Sci.* **1970**, *C4*, 110.

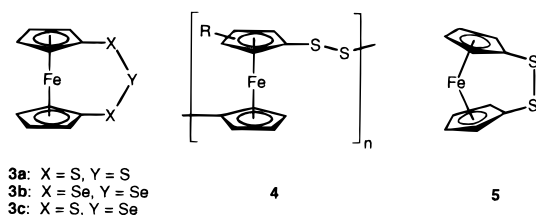
(2) Osborne, A. G.; Whiteley, R. H. *J. Organomet. Chem.* **1975**, *101*, C27.

(3) Stoeckli-Evans, H.; Osborne, A. G.; Whiteley, R. H. *Helv. Chim. Acta* **1976**, *59*, 2402.

This ROP methodology has also been extended to the synthesis of a range of other poly(metalloenes) (**2**) with germanium (E = Ge),¹⁴ phosphorus (E = P),¹⁵ tin (E = Sn),¹⁶ or two carbon atom (ER_x = C₂R₄ or C₂H₂)^{17–19} spacers, and recent attention has also focused on the interesting properties of these and related materials.^{20–22} In particular, the nature of the spacer group ER_x has been found to control the metal–metal interactions present. For example, cyclic voltammetric studies have revealed that poly(ferrocenylsilanes) **2** (ER_x = SiR₂) exhibit substantial redox-coupling ($\Delta E = 0.21–0.27$ V) whereas for poly(ferrocenylethylenes) **2** (ER_x = C₂H₄), which possess a more insulating hydrocarbon bridge, the metal–metal interactions are small ($\Delta E = 0.09$ V).^{18,23,24} Understanding and control of the metal–metal interactions in poly(metalloenes) **2** is likely to be an important factor for the further exploitation of the interesting charge transport and cooperative magnetic properties which have been reported for these materials.^{18,20c,21c}

To date, [1]ferrocenophanes **1** with group 14 (E = Si, Ge, Sn), group 15 (E = P, As), and group 4 (E = Ti, Zr, Hf) bridging elements have been prepared and characterized.²⁵ The strain present in these species is apparent in the characteristic tilt-angles which range from 6° (E = Zr) to 27° (E = P). [1]Ferrocenophanes containing group 16 elements such as sulfur in the bridge which possess small covalent radii would be expected to possess even more strained, ring-tilted structures than their groups 14 and 15 analogs.²⁶ Prior to the initiation of the research described in this paper, [1]chalcogenoferrocenophanes were unknown. However, trithia-bridged [3]ferrocenophanes such as **3a** have been well-studied and have

previously been prepared from the reactions of dilithiated ferrocenes with elemental sulfur.²⁷ Triseleno-, tritellura- and



(9) Rulkens, R.; Ni, Y.; Manners, I. *J. Am. Chem. Soc.* **1994**, *116*, 12121.

(10) Ni, Y.; Rulkens, R.; Manners, I. *J. Am. Chem. Soc.* **1996**, *118*, 4102.

(11) Ni, Y.; Rulkens, R.; Pudelski, J. K.; Manners, I. *Macromol. Rapid Commun.* **1995**, *16*, 637.

(12) Reddy, N. P.; Yamashita, H.; Tanaka, M. *J. Chem. Soc., Chem. Commun.* **1995**, 2263.

(13) Gómez-Elipe, P.; Macdonald, P. M.; Manners, I. *Angew. Chem., Int. Ed. Engl.* **1997**, *36*, 762.

(14) Foucher, D. A.; Edwards, M.; Burrow, R. A.; Lough, A. J.; Manners, I. *Organometallics* **1994**, *13*, 4959.

(15) Honeyman, C. H.; Foucher, D. A.; Dahmen, F. Y.; Rulkens, R.; Lough, A. J.; Manners, I. *Organometallics* **1995**, *14*, 5503.

(16) Rulkens, R.; Lough, A. J.; Manners, I. *Angew. Chem., Int. Ed. Engl.* **1996**, *35*, 1805.

(17) Nelson, J. M.; Rengel, H.; Manners, I. *J. Am. Chem. Soc.* **1993**, *115*, 7035.

(18) Nelson, J. M.; Nguyen, P.; Petersen, R.; Rengel, H.; Macdonald, P. M.; Lough, A. J.; Manners, I.; Raju, N. P.; Greedan, J. E.; Barlow, S.; O'Hare, D. *Chem. Eur. J.* **1997**, *3*, 573.

(19) Buretea, M. A.; Tilley, T. D. *Organometallics* **1997**, *16*, 1507.

(20) For example, see: (a) Foucher, D. A.; Ziembinski, R.; Tang, B.-Z.; Macdonald, P. M.; Massey, J.; Jaeger, C. R.; Vancso, G. J.; Manners, I. *Macromolecules* **1993**, *26*, 2878. (b) Foucher, D.; Ziembinski, R.; Petersen, R.; Pudelski, J.; Edwards, M.; Ni, Y.; Massey, J.; Jaeger, C. R.; Vancso, G. J.; Manners, I. *Macromolecules* **1994**, *27*, 3992. (c) Manners, I. *Adv. Organomet. Chem.* **1995**, *37*, 131. (d) Liu, X.-H.; Bruce, D. W.; Manners, I. *J. Chem. Soc., Chem. Commun.* **1997**, 289.

(21) (a) Nguyen, M. T.; Diaz, A. F.; Dement'ev, V. V.; Pannell, K. H. *Chem. Mater.* **1993**, *5*, 1389. (b) Nguyen, M. T.; Diaz, A. F.; Dement'ev, V. V.; Pannell, K. H. *Chem. Mater.* **1994**, *6*, 952. (c) Hmyene, M.; Yassar, A.; Escorne, M.; Percheron-Guegan, A.; Garnier, F. *Adv. Mater.* **1994**, *6*, 564. (d) Barlow, S.; Rohl, A. L.; Shi, S.; Freeman, C. M.; O'Hare, D. *J. Am. Chem. Soc.* **1996**, *118*, 7578.

(22) For recent work on other poly(ferrocenes), see: (a) Bayer, R.; Pöhlmann, T.; Nuyken, O. *Makromol. Chem. Rapid Commun.* **1993**, *14*, 359. (b) Rosenblum, M.; Nugent, H. M.; Jang, K.-S.; Labes, M. M.; Cahalane, W.; Klemarczyk, P.; Reiff, W. M. *Macromolecules* **1995**, *28*, 6330. (c) Morán, M.; Pascual, M. C.; Cuadrado, I.; Losada, J. *Organometallics* **1993**, *12*, 811. (d) Stanton, C. E.; Lee, T. R.; Grubbs, R. H.; Lewis, N. S.; Pudelski, J. K.; Callstrom, M. R.; Erickson, M. S.; McLaughlin, M. L. *Macromolecules* **1995**, *28*, 8713. (e) Galloway, C. P.; Rauchfuss, T. B. *Angew. Chem., Int. Ed. Engl.* **1993**, *32*, 1319.

(23) Foucher, D. A.; Honeyman, C. H.; Nelson, J. M.; Tang, B.-Z.; Manners, I. *Angew. Chem., Int. Ed. Engl.* **1993**, *32*, 1709.

(24) Rulkens, R.; Lough, A. J.; Manners, I.; Lovelace, S. R.; Grant, C.; Geiger, W. E. *J. Am. Chem. Soc.* **1996**, *118*, 12683.

(25) Herberhold, M. *Angew. Chem., Int. Ed. Engl.* **1995**, *34*, 1837.

mixed chalcogeno-bridged [3]ferrocenophanes have been synthesized by similar routes.^{28,29} As these species are essentially unstrained (tilt-angles < 4.5°), they appear to be unsuitable monomers for ROP. Nevertheless, Rauchfuss and co-workers have shown that these compounds undergo novel sulfur atom abstraction-induced polymerization reactions with PBu₃ to give poly(ferrocenyl persulfides) **4**.³⁰ Strained dithio-bridged [2]ferrocenophanes **5** have been proposed as possible intermediates in these polymerizations but have not been identified or isolated to date.^{30–32}

Significantly, cyclic voltammetric studies of poly(ferrocenyl persulfides) **4** have shown the presence of strong metal–metal interactions [$\Delta E = 0.29–0.31$ V] despite the existence of a two atom spacer between the ferrocene units.^{31,32} This discovery provided further motivation for us to study ring-opened polymers derived from [1]chalcogenoferrocenophanes. In this paper, as a follow up to our communication,³³ we report full details concerning both the synthesis of the first stable [1]chalcogenoferrocenophanes and studies of the ROP behavior of these species.

Results and Discussion

Synthesis and Characterization of the Sulfur-Bridged [1]-

Ferrocenophane Fe(η -C₅H₄)₂S (6**).** Attempts to prepare a sulfur-bridged [1]ferrocenophane (**6**) via the low-temperature reaction of dilithioferrocene·tetramethylethylenediamine [fLi₂·TMEDA] with SCl₂ yielded only chlorinated ferrocenes and uncharacterized byproducts. An alternative approach involved the low-temperature reaction of fLi₂·TMEDA with S(O₂SPh)₂ in THF. A critical step in the reaction was the removal of the partially THF soluble Li[O₂SPh] byproduct, which was found to induce decomposition of the product **6** presumably via ring-opening oligomerization reactions.³⁴ This separation was achieved by addition of cold hexanes to the reaction mixture and subsequent low temperature (–78 °C) filtration through alumina. A second filtration through alumina and column chromatography followed by sublimation of the product afforded a purple solid contaminated with a trace quantity of ferrocene (<5% by ¹H NMR) in 56% yield. Recrystallization from

(26) Single-bond covalent radii (Si, 1.17 Å; P, 1.12 Å; S, 1.02 Å) and covalent single-bond distances (Si–C, 1.87 Å; P–C, 1.84 Å; S–C, 1.82 Å) suggest that sulfur would represent the smallest element incorporated into the bridge of a [1]ferrocenophane. See: Jolly, W. L. *The Principles of Inorganic Chemistry*; McGraw-Hill: New York, 1976; Chapter 2.

(27) Bishop, J. J.; Davison, A.; Katcher, M. L.; Lichtenberg, D. W.; Merrill, R. E.; Smart, J. C. *J. Organomet. Chem.* **1971**, *27*, 241.

(28) Osborne, A. G.; Hollands, R. E.; Howard, J. A. K.; Bryan, R. F. *J. Organomet. Chem.* **1981**, *205*, 395.

(29) Herberhold, M.; Leitner, P.; Thewalt, U. *Z. Naturforsch.* **1990**, *45b*, 1503.

(30) Brandt, P. F.; Rauchfuss, T. B. *J. Am. Chem. Soc.* **1992**, *114*, 1926.

(31) Compton, D. L.; Rauchfuss, T. B. *Organometallics* **1994**, *13*, 4367.

(32) Compton, D. L.; Brandt, P. F.; Rauchfuss, T. B.; Rosenbaum, D. F.; Zukoski, C. F. *Chem. Mater.* **1995**, *7*, 2342.

(33) Pudelski, J. K.; Gates, D. P.; Rulkens, R.; Lough, A. J.; Manners, I. *Angew. Chem., Int. Ed. Engl.* **1995**, *34*, 1506.

(34) When a small amount of Li[O₂SPh] was added to a solution of pure **6** in C₆D₆, immediate precipitation of a brown solid was observed.

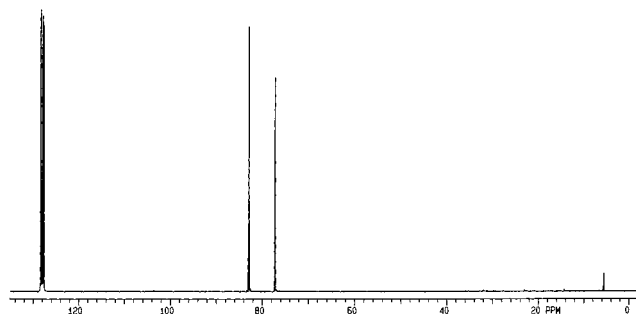


Figure 2. ^{13}C NMR spectrum of **7** in C_6D_6 .

(ca. 91°). The S–C bond lengths (av $1.806(3)$ Å) are typical of S–C single bonds, although they are slightly elongated relative to analogous bonds in the trithia-bridged [3]ferrocenophane **3a** (ca. 1.75 – 1.76 Å). The distance between Fe and the bridging S atom [$2.7947(7)$ Å] is slightly longer than that expected for a single bond (sum of covalent radii = 2.27 Å)³⁹ and is consistent with the type of weak interaction previously proposed for [1]ferrocenophanes.^{4–6}

Synthesis and Structure of the Selenium-Bridged [1]-Ferrocenophane $\text{Fe}(\eta\text{-C}_5\text{H}_4)_2\text{Se}$ (7**).** Initial attempts to prepare the selenium-bridged species **7** by a procedure analogous to that for **6** via the low-temperature reaction of $\text{Se}(\text{O}_2\text{SPh})_2$ and $\text{fcLi}_2 \cdot \text{TMEDA}$ resulted in the formation of very low yields of the product. Substantially improved yields were obtained by a similar procedure using selenium bis(diethylthiocarbamate), $\text{Se}(\text{S}_2\text{CNEt}_2)_2$, in place of $\text{Se}(\text{O}_2\text{SPh})_2$. In addition to the desired product **7**, a quantity of yellow-brown insoluble material was produced, which can be attributed to the anionic ring-opening oligomerization of **7**, initiated by the lithium salt of the selenium ligand, $\text{Li}[\text{S}_2\text{CNEt}_2]$, produced during the reaction. The challenge of isolation for **7** is more pronounced than that for **6**, at least partly caused by the increased solubility of the $[\text{S}_2\text{CNEt}_2]^-$ anion in the reaction solvent. Thus, a similar low-temperature filtration through alumina was required to remove $\text{Li}[\text{S}_2\text{CNEt}_2]$ and allow workup of **7** under ambient conditions. The selenium-bridged [1]ferrocenophane **7** was isolated by recrystallization from hexanes followed by vacuum sublimation to afford red-purple crystals, free from ferrocene, in 23% yield. Once isolated and free from impurities, **7** was found to be stable at room temperature in both the solid state and in solution in the absence of air and moisture.

It is interesting to note that **7** can also be prepared by the abstraction of selenium from the [3]ferrocenophane **3c** by dilithioferrocene. If due caution is taken to reduce anionic oligomerization via the addition of Me_3SiCl to the reaction mixture, low yields of **7** can be obtained via this method.

Compound **7** was characterized by mass spectrometry and by ^1H , ^{13}C , and ^{77}Se NMR spectroscopies. The ^1H NMR spectrum of **7** in C_6D_6 showed two pseudotriplets which were less separated than for **6** ($\Delta\delta = 0.62$ vs 0.65 ppm for **6**). In the ^{13}C NMR spectrum (Figure 2) of **7**, three resonances were observed for the Cp carbons, and in particular, the signal for the *ipso*-carbon atom was found at 5.6 ppm, which is surprisingly further upfield than that of **6** (14.3 ppm). The ^{77}Se NMR spectrum showed a singlet at 435 ppm, which is shifted slightly downfield from the resonance observed in diaryl selenides such as Ph_2Se (402 ppm)⁴⁰ and dramatically shifted downfield with respect to the ^{77}Se resonance $\text{C}_5\text{H}_4\text{Se}$ in **3b** (303 ppm).³² Cyclic voltammetric analysis of **7** showed a reversible oxidation at scan

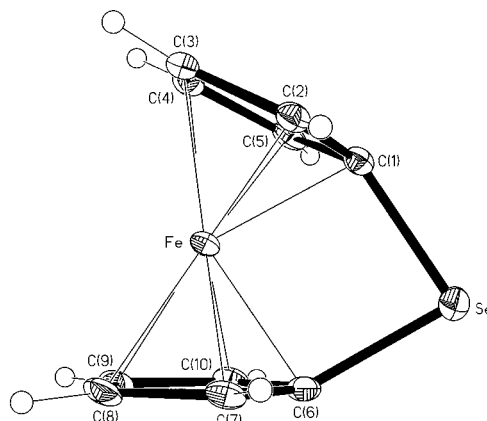


Figure 3. Molecular structure of **7** with thermal ellipsoids shown at the 30% probability level.

rates above 50 mV/s, in contrast to that of **6** which was shown to be reversible only at scan rates greater than 500 mV/s. The half-wave oxidation potential for **7** was found to be -0.02 V at a scan rate of 250 mV/s, which is typical for [1]silaferrocenophanes.⁶

A single crystal suitable for an X-ray diffraction study was obtained by slow solvent evaporation of a benzene solution of **7**. The molecular structure is shown in Figure 3 and reveals a ring-tilt (α) of $26.4(2)^\circ$, which reflects the strain present in **7** and is substantially greater than that found in the analogous, fourth row element containing arsenic- (22.9°) or germanium- [$19.0(9)^\circ$] bridged [1]ferrocenophanes (Table 1), although expectedly is significantly less than in **6** [$\alpha = 31.05(10)^\circ$].⁴¹ It is interesting to note that the β angles in **7** are slightly larger than those in **6** (av $30.0(2)^\circ$ vs $29.0(2)^\circ$, respectively) which may be a factor in the upfield shift of the *ipso*-carbon resonance in the ^{13}C NMR spectrum (Table 1). Another striking feature in the molecular structure of **7** is the C1–Se–C6 angle of $86.00(12)^\circ$ which is approximately 3° less than the corresponding angle in **6** ($89.03(9)^\circ$). As for **6**, the distance between Fe and the bridging atom ($2.9058(6)$ Å) is possibly consistent with a weak interaction (sum of covalent radii = 2.42 Å).

Now that the series is completed, a general trend in the structural features of main-group-containing [1]ferrocenophanes should be pointed out (see Table 1). Whereas the tilt-angle (α) increases dramatically on traversing each period ($n = 3$ and 4) from group 14 to 16, the other angles β , δ , and θ undergo a smooth decrease.

The Electronic Structure of [1]Ferrocenophanes; UV/Vis Spectra and Extended Hückel MO Calculations. In order to obtain information on the electronic structure of the chalcogen-bridged [1]ferrocenophanes, solution UV/vis spectra in the 200–800 nm range were collected for species **6** and **7**. In hexanes, **6** exhibits UV/vis absorbances at 275, 322, and 504 nm (Figure 4), while **7** shows absorbances at 273, 328, and 500 nm. In comparison to the UV/vis spectrum of ferrocene, these bands are assigned the numbers IV, III, and II, respectively. The two highest energy bands IV and III occur at a similar energy to those in ferrocene, whereas the lowest energy band II is dramatically red-shifted by ca. 60 nm. In addition, both bands III and II are significantly more intense than the corresponding absorptions in ferrocene (see Figure 4, Table 1). An analogous but less significant red-shift (ca. 40 nm) of the lowest energy band II has been detected for silicon-bridged ferrocenes which possess smaller tilt-angles (16 – 21°).⁶ These shifts of band II give rise to the characteristic amber color of

(39) Huheey, J. E.; Keiter, E. A.; Keiter, R. L. *Inorganic Chemistry*, 4th ed.; Harper Collins: New York, 1993; p 292.

(40) McFarlane, H. C. E.; McFarlane, W. In *NMR of Newly Accessible Nuclei*; Laslo, P., Ed.; Academic Press: London, 1983; Vol. 2, p 275.

(41) Single-bond covalent radii (Ge, 1.22 ; As, 1.22 Å; Se, 1.17 Å). See ref 39.

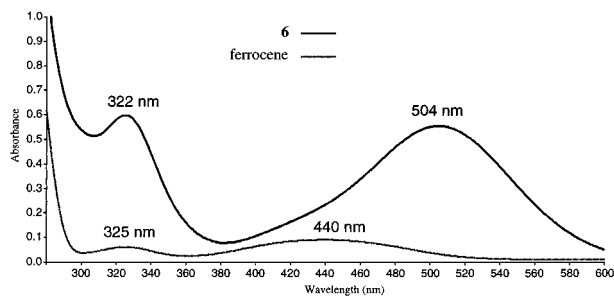


Figure 4. UV/vis spectra of ferrocene (bottom) and **6** (top) (1.0 mM solutions in hexanes).

ferrocene, the red color of silicon-bridged [1]ferrocenophanes, and, as noted above, the remarkable purple color of the sulfur-bridged [1]ferrocenophane **6**.

In order to probe the reasons for the dramatic red-shift of the lowest energy band which leads to the striking purple color of **6** we have performed some extended Hückel MO (EHMO) calculations on some representative structures with the CACAO program.

First, the electronic structure for ferrocene in the eclipsed (D_{5h}) configuration was generated and was found to give satisfactory agreement with the accepted order of energy levels which give rise to a ground state arising from an $e''_4a_1'^2$ electronic configuration.⁴² Calculations were then performed on the silicon-bridged [1]ferrocenophane **1** ($ER_x = SiH_2$) (tilt-angle 19.1°)⁴³ and the sulfur-bridged species **6** (tilt-angle 31.05°) using the X-ray crystallographic data to define the (eclipsed) molecular structures. A calculation on ferrocene with rings tilted by the same value as in **6** (31.05°) in the absence of a bridging atom was also performed. Energy level diagrams showing the frontier molecular orbitals are illustrated in Figures 5 and 6.

The highest energy UV/vis absorption in ferrocene (band IV) at 270 nm has been assigned to a ligand-to-metal charge transfer transition, whereas the weaker absorptions at 325 and 440 nm (bands III and II) have been attributed to transitions between the filled e' and a_1' HOMOs and the e'' LUMO, which are predominantly d–d in nature and Laporte forbidden. The absorption at 440 nm has been assigned to two closely spaced absorptions (band IIa and IIb) of which the lowest energy component (IIa), i.e., the component that undergoes the dramatic red-shift in [1]ferrocenophanes (see Figure 4), has been assigned to a one electron $a_1' \rightarrow e''$ transition. Inspection of Figure 6 shows that the HOMO–LUMO gap (corresponding to the gap between the a_1' level and the e'' level in ferrocene) decreases significantly as the tilt-angle increases, i.e., the a_1' HOMO is raised in energy whereas the LUMO energy is lowered. In addition, as the e' -occupied MO (which becomes a_1 and b_1 in the tilted structures) remains at relatively constant energy, the large percentage change in the HOMO (a_1')–LUMO gap explains, at least qualitatively, why the lowest energy transition (IIa) is the one to red-shift most dramatically with increasing ring-tilt.⁴⁴ The greater intensity of bands III and II can be explained by the relaxation of the Laporte selection rule as the symmetry is lowered by increased tilting and the increased cyclopentadienyl ligand contribution to the LUMOs.

Another interesting structural question concerning strained metallocenophanes involves the possible existence of a weak

dative bond between the iron atom and the bridging element. In all structurally characterized [1]ferrocenophanes reported to date, the distance between the iron atom and the bridging element is only slightly (typically ca. 10–20%) longer than that for a single bond. Moreover, ^{57}Fe Mössbauer spectroscopic studies have also provided some apparently convincing support for the presence of such an interaction.⁴⁵ As Figures 5 and 6 illustrate, we found that the program used in this work generates essentially the same MO diagram for ferrocene, which is tilted by 31.05° , as for the sulfur-bridged species **6**. This indicates that the presence of a bridging element does not significantly influence the frontier orbital situation. However, we believe that higher level calculations than those reported here are required to address the issue of the possible existence of a iron-bridging element interaction in detail.

Thermal ROP of Fe(η -C₅H₄)₂S (6**) and Fe(η -C₅H₄)₂Se (**7**).** Since **6** possesses a highly strained structure, thermal ROP was expected to result in the formation of the poly(ferrocenyl sulfide) **8**. Differential scanning calorimetry (DSC) studies of **6** show an endotherm corresponding to a melt at $80^\circ C$ and a sharp exotherm at ca. $140^\circ C$ corresponding to a ring-opening process. An estimation of the enthalpy for the ROP process was made on the basis of the integration of the exotherm and was found to be ca. $130(\pm 20)$ kJ/mol. This is substantially higher than the values found for silicon-bridged [1]ferrocenophanes **1** ($ER_x = SiR_2$) (70 – 80 kJ/mol).^{8,46} An attempt to polymerize **6** on a preparative scale was carried out by heating the sulfur-bridged [1]ferrocenophane at $150^\circ C$ for 30 min after which time a beige solid product was obtained. This product was found to be insoluble in common solvents, and no useful NMR spectroscopic or molecular weight data could be obtained. However, pyrolysis mass spectrometry of this solid provided evidence for the expected structure and showed ions assigned to oligo(ferrocenyl sulfides) of up to 4 repeat units. The IR spectrum of this material was similar to that of the briefly reported poly(ferrocenyl sulfide) **8** prepared by condensation methods from fLi_2 and $SnCl_2$.⁴⁷

A DSC study of **7** (Figure 7) revealed a slight melt endotherm (observed in one of three identical samples) followed immediately by a very sharp exotherm at ca. $130^\circ C$ corresponding to a ring-opening process. Integration of the DSC exotherm gave an enthalpy for the ROP process of $110(\pm 20)$ kJ/mol, which is expectedly less than that of **6**. An attempt to polymerize **7** was carried out by heating the selenium-bridged [1]ferrocenophane *in vacuo* at $150^\circ C$ for 45 min. A beige-brown solid product (**9**) was isolated and found to be similarly insoluble in common solvents. Pyrolysis mass spectrometry of this material showed peaks assigned to oligo(ferrocenyl selenides) of up to 3 repeat units. In addition, the IR spectrum of this material was very similar to that of the insoluble poly(ferrocenyl sulfide) **8**.

Anionic Oligomerization and Attempted Anionic Polymerization of Sulfur-Bridged [1]Ferrocenophane Fe(η -C₅H₄)₂S (6**).** Anionic ROP of silicon-bridged [1]ferrocenophanes provides a convenient and well-established route to poly(ferrocenylsilanes) (**2**, $ER_x = SiR_2$) with controlled structures.¹⁰ In an attempt to synthesize poly(ferrocenyl sulfides) under mild conditions and in solution, the reaction of **6** with the anionic initiators butyllithium and dilithioferrocene·TMEDA were studied. With small amounts of BuLi in THF, an insoluble orange precipitate of the poly(ferrocenyl sulfide) **8** formed over

(42) Sohn, Y. S.; Hendrickson, D. N.; Gray, H. B. *J. Am. Chem. Soc.* **1971**, *93*, 3603.

(43) Pudelski, J. K.; Rulkens, R.; Foucher, D. A.; Lough, A. J.; Macdonald, P. M.; Manners, I. *Macromolecules* **1995**, *28*, 7301.

(44) The predicted reduction in the HOMO–LUMO and HOMO–1–LUMO gap on tilting ferrocene to $\alpha = 31^\circ$ is ca. 45% for the a_1' HOMO and ca. 15% for the e'/b_1 MO, respectively.

(45) Silver, J. J. *Chem. Soc., Dalton Trans.* **1990**, 3513.

(46) Pudelski, J. K.; Foucher, D. A.; Honeyman, C. H.; Macdonald, P. M.; Manners, I.; Barlow, S.; O'Hare, D. *Macromolecules* **1996**, *29*, 1894.

(47) Chien, J. C. W.; Gooding, R. D.; Lilly, C. P. *Polym. Mater. Sci. Eng.* **1983**, *49*, 107.

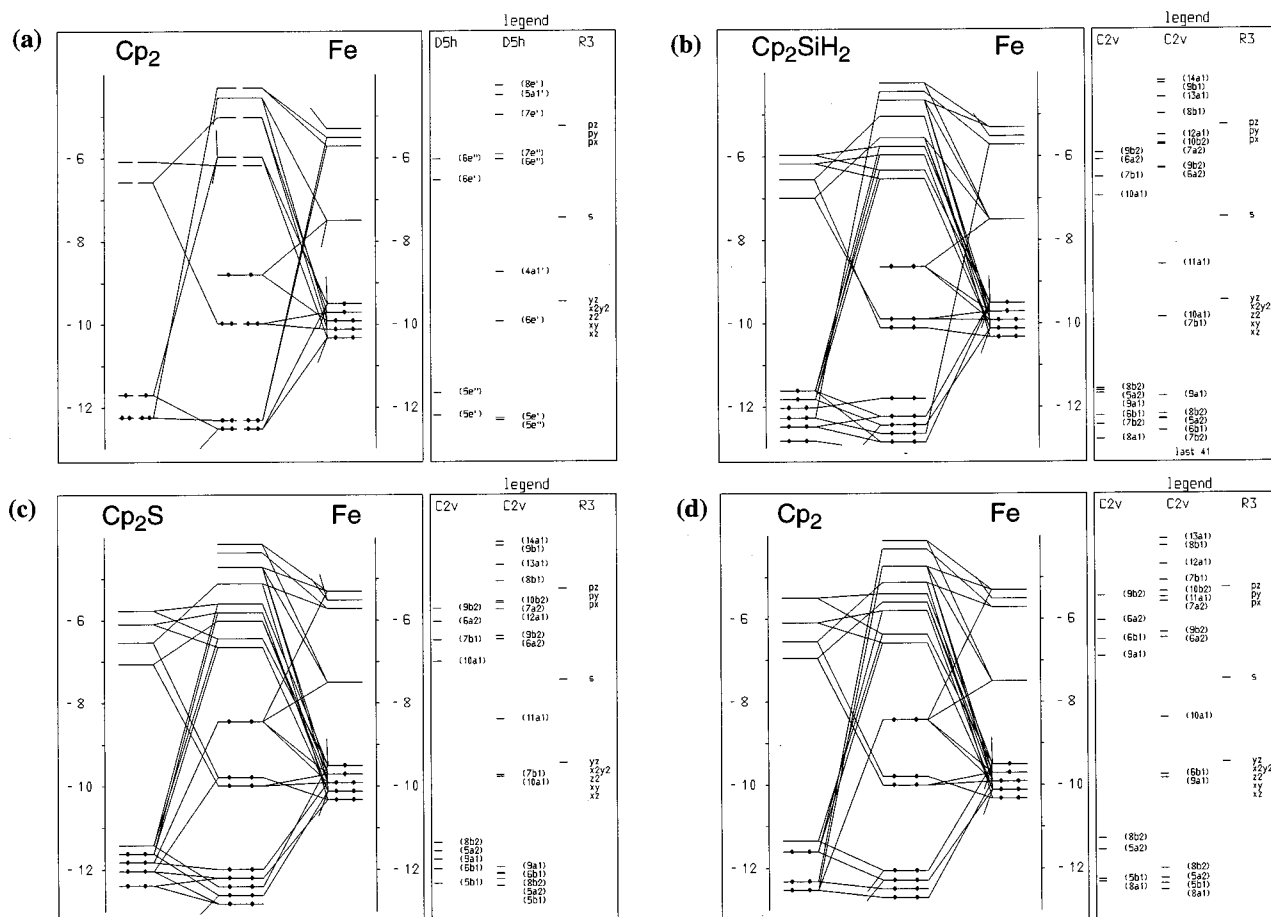


Figure 5. Interaction diagrams from EHMO calculations: (a) ferrocene (eclipsed), (b) **1** ($ER_x = \text{SiH}_2$) ($\alpha = 19.1^\circ$), (c) **6** ($\alpha = 31.05^\circ$), (d) ferrocene ($\alpha = 31.05^\circ$) (correct orbital energies in eV are given in the legend).

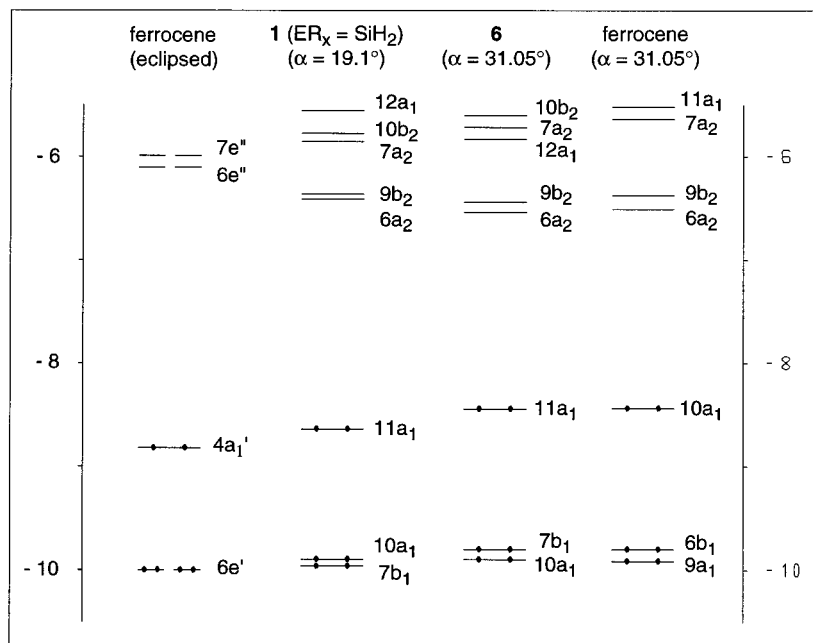


Figure 6. EHMO comparison of frontier orbitals of ferrocene (eclipsed), **1** ($ER_x = \text{SiH}_2$) ($\alpha = 19.1^\circ$), **6** ($\alpha = 31.05^\circ$), and ferrocene ($\alpha = 31.05^\circ$). Energies are given in eV.

3 d. This insoluble material is similar to that formed by the thermal treatment of **6** and that reported from the polycondensation of dilithioferrocene·TMEDA and SCl_2 .⁴⁷ In an attempt to prepare oligomers which might prove to be more soluble, the reaction of a 1:1 mixture of dilithioferrocene·TMEDA with **6** was studied. A rapid color change from deep red to amber was observed, and after the addition of Me_3SiCl , soluble

trimethylsilyl end-capped oligo(ferrocenyl sulfides) **10b** and **11b** were isolated by column chromatography. These species were characterized by NMR spectroscopy, mass spectrometry, and cyclic voltammetry.

Cyclic voltammetry (Figure 8) found slightly larger $\Delta E_{1/2}$ values for **10b** and **11b** (ca. 0.33 and 0.52 V) than were previously reported for the analogous molecules **10a** and **11a**

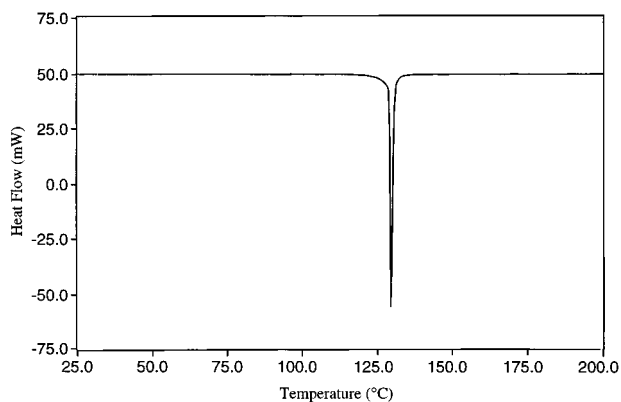


Figure 7. DSC of selenium-bridged [1]ferrocenophane **7** (10 °C/min).

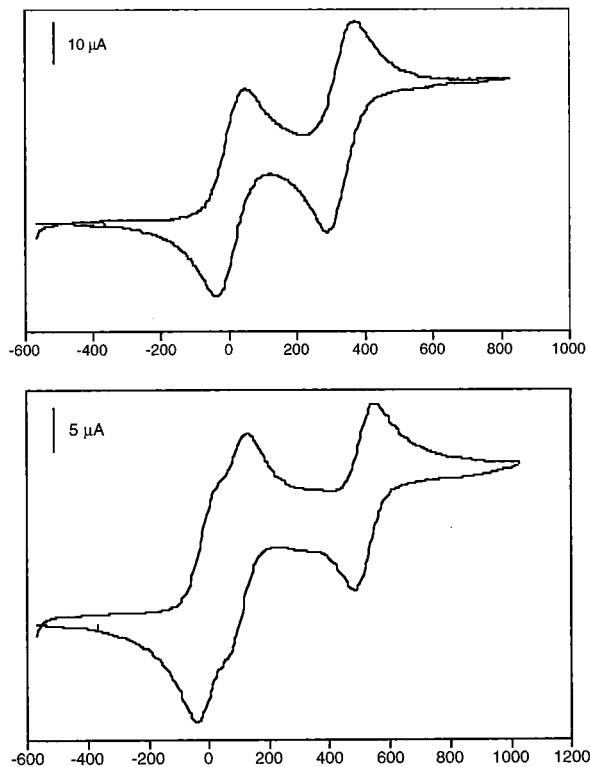
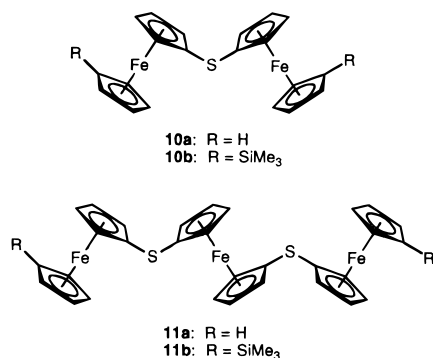


Figure 8. Cyclic voltammograms of **10b** (top) and **11b** (bottom) in CH_2Cl_2 (scan rate 250 mV/s).

(ca. 0.29 and 0.48 V)^{48–50} and which were consistent with the



presence of strong $\text{M}\cdots\text{M}$ interactions (Table 3). This is

(48) O'Conner, D. C.; Cowan, D. O. *J. Organomet. Chem.* **1991**, *408*, 227.

(49) Herberhold, M.; Brendel, H.-D.; Nuyken, O.; Pöhlmann, T. *J. Organomet. Chem.* **1991**, *413*, 65.

(50) Zanella, P.; Opromolla, G.; Herberhold, M.; Brendel, H.-D. *J. Organomet. Chem.* **1994**, *484*, 67.

Table 3. Half-Wave Potentials $E_{1/2}$ (CH_2Cl_2 vs $\text{Fe}(\eta\text{-C}_5\text{H}_5)_2^{0/+}$) and Redox Coupling ΔE for **10a**, **10b**, **11a**, and **11b**^a

compound	$E_{1/2}(1)$	$E_{1/2}(2)$	$E_{1/2}(3)$	ΔE^a	ref
10a	0.08	0.37		0.29	48
10b	0.01	0.33		0.33	this work
11a	-0.04	-0.05	0.44	0.48	50
11b	-0.01	0.09	0.51	0.52	this work

^a All values are given in volts vs $[\text{Fe}(\eta\text{-C}_5\text{H}_5)_2]^{0/+}$. ^b $\Delta E = E_{1/2}(2) - E_{1/2}(1)$ for **10a** and **10b**; $\Delta E = E_{1/2}(3) - E_{1/2}(1)$ for **11a** and **11b**.

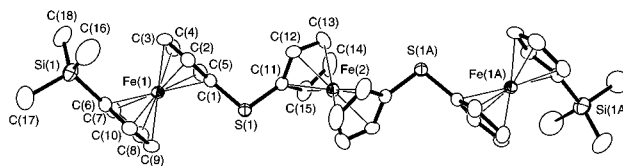


Figure 9. Molecular structure of **11b** with thermal ellipsoids shown at the 50% probability level.

supported by comparison with analogous oligo- and poly(ferrocenylsilanes) **2** ($\text{ER}_x = \text{SiMe}_2$) which exhibit smaller $\Delta E_{1/2}$ values (ca. 0.24 V).^{8,24} In addition, a clear splitting ($\Delta E = 0.10$ V) was observed for the first oxidation wave for the trimer **11b** (Figure 8), which is indicative of interactions between non-nearest-neighbor iron centers.²⁴ For the oligo(ferrocenylsilane) analog, such effects are almost undetectable.^{24,51,52}

Single crystals of **11b** were obtained by recrystallization from hexanes, and the molecular structure of **11b** was determined by single crystal X-ray diffraction (Figure 9). An interesting feature of the molecular structure of **11b** is that the triferrocenyl sulfide unit adopts an approximate *trans*-planar zigzag conformation in which the iron atoms are 6.608(1) Å apart. This compares with the analogous triferrocenylsilane in which the iron atoms are ca. 6.2 Å apart.^{52,53} The orientation of the molecules relative to one another is interesting; *intermolecular* close contacts between Cp ligands and the iron atoms make the *intermolecular* $\text{Fe}(1)\cdots\text{Fe}(2)$ distance [5.638(1) Å] significantly shorter than the *intramolecular* $\text{Fe}(1)\cdots\text{Fe}(2)$ distance [6.608(1) Å]. Similar packing effects may also be present in crystalline regions of poly(ferrocenyl sulfide) **8** which could help to explain the insolubility of this material. Similar interactions have been predicted in oligo- and poly(ferrocenylsilanes) using molecular mechanics calculations and in some cases have been verified experimentally.^{24,54}

Synthesis and Characterization of the Cp-Methylated Sulfur-Bridged [1]Ferrocenophane $\text{Fe}(\eta\text{-C}_5\text{H}_3\text{Me}_2)\text{S}$ (**12**).

The insolubility of the poly(ferrocenyl chalcogenides) **8** and **9** is not surprising as poly(ferrocenes) without flexible substituents or structural irregularity (e.g., lack of substituents on the bridging atom) tend to be insoluble in organic solvents. This effect is observed for polymer **4** (R = H) with a disulfide spacer, whereas derivatives with an alkyl group attached to the Cp ligands [e.g., **4** (R = *n*-Bu)] are soluble.³⁰ In order to obtain a ROP precursor that would be likely to form a more soluble poly(ferrocenyl sulfide), the synthesis of an isomeric mixture of the dimethyl-substituted sulfur-bridged [1]ferrocenophanes **12** was also undertaken. Due to the fact that both dilithiodimethylferrocene·TMEDA and $\text{S}(\text{O}_2\text{SPh})_2$ are fully soluble in THF ($\text{fC}_2\text{Li}_2\cdot\text{TMEDA}$ is only slightly soluble in THF at -100 °C), the

(51) Rulkens, R.; Lough, A. J.; Manners, I. *J. Am. Chem. Soc.* **1994**, *116*, 797.

(52) Pannell, K. H.; Dementiev, V. V.; Li, H.; Cervantes-Lee, F.; Nguyen, M. T.; Diaz, A. F. *Organometallics* **1994**, *13*, 3644.

(53) Lough, A. J.; Manners, I.; Rulkens, R. *Acta Crystallogr.* **1994**, *C50*, 1667.

(54) (a) Barlow, S.; Rohl, A. L.; O'Hare, D. *J. Chem. Soc., Chem. Commun.* **1996**, 257. (b) See ref 21d.

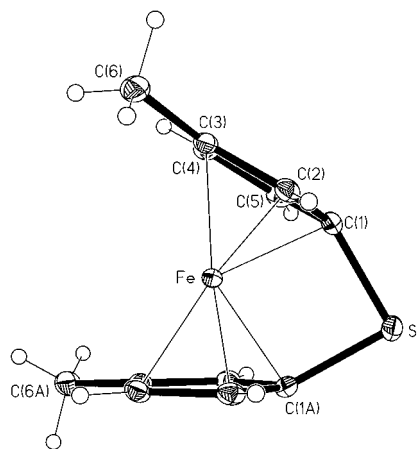
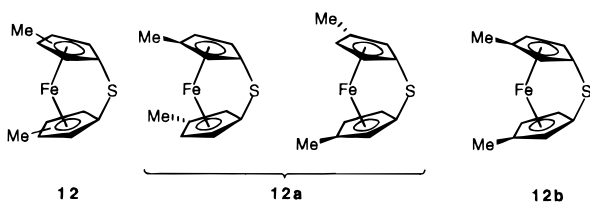


Figure 10. Molecular structure of **12a** with thermal ellipsoids shown at the 30% probability level.

reaction to form **12** in THF was found to proceed too rapidly at $-100\text{ }^{\circ}\text{C}$ and significantly lower yields were observed. Thus, diethyl ether was used as a solvent for this reaction, since $\text{S}(\text{O}_2\text{-SPh})_2$ is only slightly soluble in this solvent, and these conditions allowed the successful isolation of the isomer mixture **12** as a purple oil in 33% yield.

The enantiomer pair **12a** was separated from the mixture of isomers **12** by recrystallization from hexanes. Purple single crystals of **12a** were obtained by slow solvent evaporation from a solution in hexane. Noteworthy is the fact that the analogous procedure for the Cp-methylated dimethylsilyl-bridged [1]-ferrocenophane results in the isolation of the crystalline analog of diastereomer **12b**.⁶ The molecular structure of **12a** (Figure



10) is very similar to that of **6** and has a ring-tilt (α) of $31.46(8)^{\circ}$ which is $0.4(1)^{\circ}$ larger than that of **6**. Interestingly, this is opposite to the trend for the tilt-angles of silicon-bridged [1]-ferrocenophanes which decrease upon Cp-methylation.⁶ The β angles [$28.9(1)^{\circ}$] are comparable to those in **6**. In addition, for this species, a small staggering angle of $0.8(3)^{\circ}$ is also observed between the cyclopentadienyl ligands, implying an eclipsed conformation similar to that of the unmethylated species.

Thermal ROP of $\text{Fe}(\eta\text{-C}_5\text{H}_3\text{Me})_2\text{S}$ (12**): Synthesis and Properties of the Soluble Poly(ferrocenyl sulfide) **13**.** In an attempt to obtain a soluble poly(ferrocenyl sulfide), **12** was heated for 2 min at $160\text{ }^{\circ}\text{C}$, and the formation of a brown solid was observed accompanied by the formation of a brown cloud of smoke. Extraction of the soluble fraction into toluene, followed by filtration and precipitation into methanol, resulted in the isolation of the beige powdery poly(ferrocenyl sulfide) **13** in 50% isolated yield. The polymer was found to be soluble in benzene, toluene, and THF, but surprisingly not in CH_2Cl_2 . Analysis of **13** by ^1H NMR revealed the existence of two broad overlapping resonances in the Cp region (4.0 and 4.2 ppm) and two broad resonances in the methyl region (1.8–2.2 ppm). Gel permeation chromatography (GPC) analysis found the poly(ferrocenyl sulfide) to be of very moderate molecular weight ($M_w = 11\ 500$, $\text{PDI} = 1.95$) ($\text{DP}_w = 47$).⁵⁵ An alternative synthesis involved the thermal treatment of **8** in xylenes solution;

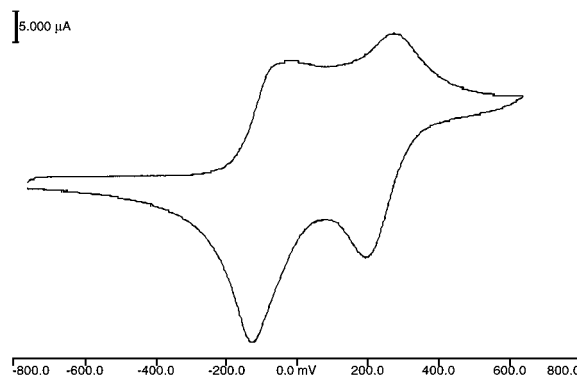
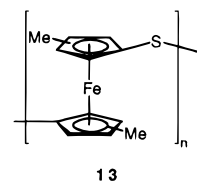


Figure 11. Cyclic voltammogram of poly(dimethylferrocenyl sulfide) **13** in THF (scan rate 25 mV/s).

however, in this case a lower yield and molecular weight was observed ($M_w = \text{ca. } 9000$, $\text{PDI} = 2.57$). The ^1H and ^{13}C NMR of this material was consistent with that of the polymer obtained by thermal ROP in the absence of solvent, and elemental analysis was consistent with the proposed structure **13**. The



IR spectrum of **13** exhibited bands similar to those of **8** and **9**. The UV/vis spectrum of **13** in hexanes showed a λ_{max} of 430 nm which is blue-shifted with respect to dimethylferrocene ($\lambda_{\text{max}} = 438\text{ nm}$), opposite to the situation for Cp-methylated poly(ferrocenylsilanes) which exhibit a red-shift from dimethylferrocene.⁴⁶

The formation of a soluble poly(ferrocenyl sulfide) allowed us to probe the metal–metal interactions present in these materials by cyclic voltammetry. Studies in THF showed two reversible oxidation waves at ca. -0.07 and ca. 0.24 V relative to ferrocene (Figure 11). The redox coupling of ca. 0.32 V (av) is considerably larger than that of **2** ($M = \text{Fe}$, $\text{ER}_x = \text{SiMe}_2$) for which a value of 0.24 V has been established, but is similar to that of a substituted poly(ferrocenyl persulfides) **4** ($R = n\text{-Bu}$, $t\text{-Bu}$), for which a redox coupling of $0.29\text{--}0.31\text{ V}$ was found in CH_2Cl_2 .^{30–32} The thermal stability of **13** was also investigated by thermogravimetric analysis (TGA). Studies showed a weight loss of about 20% between 300 and $400\text{ }^{\circ}\text{C}$ and a further weight loss beginning at $480\text{ }^{\circ}\text{C}$, giving a ceramic yield of 35% at $600\text{ }^{\circ}\text{C}$.

Anionic polymerization of **12** was also attempted. For anionic ROP to be successful, pure samples of monomer are vital. For this reason, samples of compound **12** were repeatedly subject to purification by column chromatography to remove dimethylferrocene. However traces of this species (and other impurities) could not be completely removed and were still detectable by ^1H NMR. Nevertheless, when BuLi was added as initiator, after 2 d no trace of monomer was left and the resulting beige polymer was shown to be identical with the thermally ring-opened polymer **13** by ^1H NMR. However, as expected in view of the impure nature of the monomer, analysis by GPC showed the material to be of low molecular weight ($M_w = 4300$, $\text{PDI} = 1.23$).

(55) It has, however, been shown for several poly(ferrocenylsilanes) that GPC underestimates the true molecular weight by ca. 30%. See refs 20a and b.

Thermal ROP of sulfur-bridged [1]ferrocenophanes such as **12** appears to be a less convenient route to high molecular weight poly(ferrocenes) than for group 14 element-bridged [1]ferrocenophanes, which readily afford polymers with $M_w > 10^6$, $M_n > 10^5$.⁸ The more strained nature of the sulfur-bridged species appears to lead to rather uncontrolled thermal ROP processes with more facile chain termination, which, on the basis of the isolation of some insoluble material for **12**, may also lead to some crosslinking. Future work will therefore target the preparation of high molecular weight poly(ferrocenyl sulfides) using synthetic routes such as the anionic ROP of analogs of **12** with different substituents on the Cp rings which permit more facile monomer purification. This would permit detailed studies of the physical properties of these interesting materials.

Summary

The first sulfur- and selenium-bridged [1]ferrocenophanes have been synthesized, and these remarkable species have been shown to possess tilt-angles of ca. 31° and 26°, respectively. Further evidence for the presence of a high degree of ring-strain was provided by the high-field ¹³C NMR chemical shifts of the *ipso*-carbon atoms of these [1]chalcogenoferrocenophanes. DSC analysis indicated that the strain energy for the sulfur-bridged species **6** was ca. 130(±20) kJ mol⁻¹, whereas for the selenium analog **7** the value was ca. 110(±20) kJ mol⁻¹. The red-shift detected for the lowest energy electronic transition by UV/vis spectroscopy for tilted [1]ferrocenophanes relative to ferrocene was explained by EHMO calculations which predicted a decreased HOMO–LUMO gap as the planes of the Cp ligands become more tilted. Attempts to synthesize poly(ferrocenyl sulfides) or poly(ferrocenyl selenides) by thermal or anionic ROP of unsubstituted [1]chalcogenoferrocenophanes resulted only in insoluble polymeric materials. However, soluble oligomers were obtained from 1:1 reactions of **6** with fLi₂·TMEDA followed by reactions with Me₃SiCl. The first soluble poly(ferrocenyl sulfide) **13** was synthesized by ROP of the Cp-methylated [1]thiaferrocenophane **12** and was found to be of moderate molecular weight by GPC. Cyclic voltammetric studies on oligo(ferrocenyl sulfides) and on the Cp-methylated poly(ferrocenyl sulfide) **13** showed that the Fe···Fe interactions in these materials are significantly stronger than for the corresponding oligo- or poly(ferrocenylsilanes) **2** (ER_x = SiMe₂). As thermal ROP appears to be a less efficient route for the formation of poly(ferrocenyl chalcogenides) than for other poly(metallocenes), future work will focus on (e.g., anionic) ROP of more readily purifiable analogs of **12** under mild conditions which should yield higher molecular weight materials. At that stage detailed studies of the physical properties of these materials will be made.

Experimental Section

Materials. The reagents Na[O₂SPh], Na[S₂CNEt₂], SeO₂, and Se(O)Cl₂ were purchased from Aldrich and used as received; Me₃SiCl, SiCl₂ (80%), and TMEDA were purchased from Aldrich and distilled before use. Dimethylferrocene (Aldrich) was sublimed prior to use. The starting materials S(O₂SPh)₂, S₂(O₂SPh)₂, Se(O₂SPh)₂, Se(S₂CNEt₂)₂, [3]ferrocenophane **3c**, and fLi₂·TMEDA were prepared according to the literature.^{27,28,56–58} Alumina used was purchased from BDH (activated, neutral, 100–200 mesh) or from Aldrich (activated, weakly basic, Brockmann I, 150–200 mesh). Solvents were dried by standard methods and freshly distilled under nitrogen prior to use. All

reactions were carried out under an atmosphere of prepurified nitrogen (99.999% Canox) using standard Schlenk techniques or in an inert atmosphere glovebox (Innovative Technology Inc. or Vacuum Atmospheres Co.).

Equipment. NMR spectra were recorded on Varian Gemini 200 or Varian Gemini 300 instruments. ¹H NMR spectra were referenced to residual protonated C₆D₆ at 7.15 ppm, and ¹³C NMR spectra were referenced the C₆D₆ signal at 128.0 ppm. ⁷⁷Se NMR spectra (57.2 MHz) were recorded on a Varian Gemini 300 instrument and referenced externally to Me₂Se. UV/vis spectra were obtained using a Perkin Elmer Lambda 900 UV/vis/near IR spectrophotometer in hexanes at concentrations of 1.0 mmol/L. Infrared spectra were obtained using KBr pellets on a Nicolet 205 instrument. Mass spectra were obtained with the VG 70-250S mass spectrometer operating in electron impact (EI) mode. Pyrolysis mass spectra were carried out by heating the sample probe to 600 °C. The molecular weight of the polymer **13** was estimated by gel permeation chromatography (GPC) using a Waters Associates liquid chromatograph equipped with a 510 HPLC pump, U6K injector, ultrastryragel columns with a pore size between 10³ and 10⁵ Å, and a Waters 410 differential refractometer. A flow rate of 1.0 mL/min was used, and the sample was dissolved in a solution of 0.1% tetra-*n*-butylammonium bromide in THF. Polystyrene standards were used for calibration purposes. DSC analyses were performed using a Perkin-Elmer DSC-7 or Dupont DSC 2910 differential scanning calorimeters under nitrogen at a heating rate of 10 °C/min. TGA of **13** was performed using a Perkin-Elmer TGA-7 thermogravimetric analyzer under nitrogen at a heating rate of 10 °C/min. Elemental analyses were performed by Quantitative Technologies, Inc., Whitehouse, NJ.

Electrochemical experiments were carried out at room temperature with a Model 273 potentiostat/galvanostat (EG&G Princeton Applied Research) on 1 mmol/L solutions in CH₂Cl₂ (for **6** and **7**), 1.0 mg/mL solutions in CH₂Cl₂ (for **10b** and **11b**), or a 0.5 mg/mL solution in THF (for **13**) which were 0.10 M in [NBu₄][PF₆]. A sample cell with Pt working and counter electrodes and an Ag reference electrode was used. Decamethylferrocene (or ferrocene) was added as an internal standard at the end of each experiment. Potentials are referenced to the ferrocene/ferrocenium couple (0 V) which is 0.500 V anodic relative to decamethylferrocene.

X-ray Structural Characterization. A summary of selected crystallographic data is given in Table 1. Data for all compounds were collected on a Siemens P4 diffractometer using graphite-monochromated Mo Kα radiation ($\lambda = 0.71073 \text{ \AA}$).

The structures were solved and refined using the SHELXTL/PC package.⁵⁹ Refinement was by full-matrix least-squares on F^2 using all data (negative intensities included). For each compound, the non-hydrogen atoms were refined with anisotropic thermal parameters and the hydrogen atoms were refined with isotropic thermal parameters. Molecular structures are presented with ellipsoids at a 30% probability level (for **6**, **7**, and **12a**) and 50% probability level (for **11b**).

EHMO Calculations. The extended Hückel MO calculations were performed using the CACAO software package of Mealli and Proserpio (PC version 3.0, July 1992).⁶⁰ Standard Atomic Parameters were utilized for carbon, hydrogen, sulfur, and silicon. The values used for iron were optimized through a comparison of the calculated EHMO energies with the generally accepted molecular orbital diagram for the eclipsed (D_{5h}) structure of ferrocene, which gives rise to a ground state arising from an $e^{4a_1'2}$ electronic configuration. These same parameters were then used throughout the entire set of calculations. The complete set is summarized in the Supporting Information.

CAUTION: Extreme caution must be exercised when adding solvent (THF) to the solid mixture in the preparation of monomers **6** and **7**. On rare occasions highly exothermic reactions accompanied by rapid pressure buildups have been observed upon addition of the first drop of solvent even at –196 °C.

(59) Sheldrick, D. M. Siemens Analytical X-ray Instruments Inc., Madison, Wisconsin, 1994.

(60) Mealli, C.; Proserpio, D. M. *J. Chem. Educ.* **1990**, *67*, 399.

(61) Seyferth, D.; Withers, H. P. *J. Organomet. Chem.* **1980**, *185*, C1.

(62) Butler, I. R.; Cullen, W. R.; Einstein, F. W. B.; Rettig, S. J.; Willis, A. J. *J. Organometallics* **1983**, *2*, 128.

(56) De Jong, J.; Janssen, M. J. *J. Org. Chem.* **1971**, *36*, 1645.

(57) Foss, O. *Acta Chem. Scand.* **1952**, *6*, 509.

(58) Foss, O.; Pitha, J. In *Inorganic Syntheses*; Bailar, J. C., Ed.; McGraw-Hill Inc.: New York, 1953; Vol. 4, see p 91.

Synthesis of Fe(η -C₅H₄)₂S (6**).** A solid mixture of fC₅H₄·TMEDA (2.01 g, 6.40 mmol) and (PhSO₂)₂S (2.45 g, 7.80 mmol) was cooled to -196 °C, tetrahydrofuran (ca. 75 mL) was slowly added, and the resulting solution was frozen. This was slowly melted by warming to -100 °C in an EtOH/liquid N₂ bath. The resulting orange-red reaction mixture was then kept at -80 °C (±10 °C) for 90 min during which time the reaction mixture turned a deep blood red color. Hexanes (ca. 50 mL) was added at -80 °C, and precipitation of a dark solid was observed. This was allowed to settle, and the supernatant solution was filtered through a precooled (-78 °C) glass frit containing a 4 cm pad of alumina, which was subsequently washed several times with hexanes (ca. 150 mL). The resulting deep red filtrate was concentrated *in vacuo* to 100 mL and filtered through a second alumina-containing frit and pumped to dryness leaving a purple solid. This solid was redissolved in hexanes (ca. 5 mL) and chromatographed on an alumina column (ca. 30 cm). The crude yield was 0.78 g (56 %). Recrystallization from hexanes (-40 °C) and sublimation (25 °C, 0.01 mmHg) yielded **6**, free from ferrocene, as a dark purple crystalline solid in a yield of 0.39 g (28%).

For 6: mp 80 °C; ¹H NMR (C₆D₆) δ (ppm) 4.61 (t, *J* = 2 Hz, 4H), 3.96 (t, *J* = 2 Hz, 4H); ¹³C NMR (C₆D₆) δ (ppm) 82.1 (Cp), 76.9 (Cp), 14.3 (Cp-S); UV/vis (hexanes) λ_{max} (ϵ) 504 nm (540 L cm⁻¹ mol⁻¹), 322 nm (578 L cm⁻¹ mol⁻¹); MS (EI, 70 eV) *m/z* [%] 216 [100; M⁺], 182 [9.6; M⁺ - H₂S], 160 [11; M⁺ - Fe], 128 [55; M⁺ - FeS], 56 [36; Fe⁺]; HRMS calcd for C₁₀H₈⁵⁶FeS 215.9696, found 215.9689. Anal. Calcd for C₁₀H₈FeS: C, 55.59; H, 3.73. Found: C, 54.50; H, 3.67.

Alternatively **6** can be synthesized by the reaction of fC₅H₄·TMEDA with S₂(O₂SPh)₂ by following the same reaction procedure as described above. Thus, from a reaction of 1.57 g of fC₅H₄·TMEDA (5.00 mmol) with 1.85 g of S₂(O₂SPh)₂ (5.34 mmol), 0.25 g of crude **6** (23%) was isolated.

Synthesis of Fe(η -C₅H₄)₂Se (7**).** A mixture of fC₅H₄·TMEDA (0.57 g, 1.8 mmol) in ether (100 mL) was cooled to -78 °C in a dry ice/acetone bath. A solution of Se[S₂CNEt₂]₂ (0.78 g, 2.1 mmol) in ether (50 mL) was cooled to -78 °C and was slowly added to the stirred suspension. When the addition was complete, the mixture was allowed to warm to -40 °C (±10 °C) and stirred for 1 h during which the color of the reaction mixture became reddish-brown. The solvent was quickly removed *in vacuo*, and the red-brown residue taken up in cold (-78 °C) hexanes (ca. 35 mL). This was immediately filtered through a 1 cm layer of dry alumina, and the solvent was removed *in vacuo* to yield a red residue, which was redissolved in hexanes (ca. 10 mL) and column chromatographed on alumina. The crude yield was 0.14 g (29%). Recrystallization from hexanes (-40 °C) and sublimation (25 °C, 0.01 mmHg) yielded analytically pure **7** as red-purple crystals in a yield of 0.11 g (23%).

For 7: mp = 143 °C (polym); ¹H NMR (C₆D₆) δ (ppm) 4.56 (ps t, *J* = 2 Hz, 4H), 3.94 (ps t, *J* = 2 Hz, 4H); ¹³C NMR (C₆D₆) δ (ppm) 82.8 (Cp), 77.2 (Cp), 5.6 (*ipso*-Cp); ⁷⁷Se NMR (C₆D₆) δ (ppm) 435 ppm; UV/vis (hexanes) λ_{max} (ϵ) 500 nm (325 L cm⁻¹ mol⁻¹); MS (EI, 70 eV) *m/z* [%] 264 [100; M⁺], 182 [12; M⁺ - Se], 136 [44; M⁺ - Cp₂], 128 [98; M⁺ - FeSe]; HRMS calcd for C₁₀H₈⁵⁶Fe⁸⁰Se 263.9140, found 263.9138. Anal. Calcd for C₁₀H₈FeSe: C, 45.67; H, 3.07. Found: C, 45.56; H, 2.81.

Alternatively, **7** can be synthesized in very low yield of the crude product by the reaction of dilithioferrocene·TMEDA with Se(O₂SPh)₂ by following the same reaction procedure as for **6**. Thus, from a reaction of fC₅H₄·TMEDA (2.5 g, 8.0 mmol) with Se(O₂SPh)₂ (3.0 g, 8.3 mmol), 0.01 g of crude **7** (0.4%) was isolated.

Low yields of **7** were also obtained by the reaction of dilithioferrocene·TMEDA and the [3]ferrocenophane **3c**. fC₅H₄·TMEDA (0.46 g, 1.5 mmol) was slurried in ether (10 mL) and frozen at -196 °C. A solution of **3c** (0.52 g, 1.59 mmol) in ether (40 mL) was slowly added, and upon completion, the mixture was allowed to melt at -110 °C. Once the mixture had melted, the temperature was increased and was held at -85 °C (±5 °C) for 2 h, during which both a red solid and a fluffy yellow precipitate formed. Me₃SiCl (0.405 mL, 3.19 mmol) was added, and the mixture allowed to warm to 25 °C. The reaction mixture was filtered, and the solvent removed *in vacuo* to yield a yellow-red solid. This was then redissolved in hexanes (50 mL) and

filtered to remove the insoluble yellow precipitate. Removal of the solvent resulted in the isolation of crude **7** (20 mg, 5%).

Thermal ROP of 6 and 7. A Pyrex polymerization tube was charged with **6** (0.10 g, 0.46 mmol), sealed under vacuum, and heated in a polymerization oven (150 °C, 30 min). This resulted in the quantitative formation of a beige insoluble powder, poly(ferrocenyl sulfide) **8**. A similar experiment with **7** yielded the beige insoluble polymer **9**.

Solubility tests on **8** and **9** were undertaken in the following solvents: THF, hexanes, acetone, ethanol, methanol, 2-propanol, benzene, toluene, xylene, DMF, DMSO, chloroform, dichloromethane, carbon tetrachloride, CS₂, and chlorobenzene. No evidence of significant solubility was observed even at elevated temperatures.

For 8: IR (cm⁻¹) 3087 (vw), 1413 (w), 1385 (w), 1354 (w), 1167 (w), 1021 (m), 885 (m), 821 (m), 512 (s), 491 (s); pyrolysis MS [fc = Fe(η -C₅H₄)₂, Fc = Fe(η -C₅H₅)(η -C₅H₄)] (EI, 70 eV) *m/z* [%] (ca. 525 °C) 864 [2; (fcS)₄⁺], 832 [25; (fcS)₄⁺ - S], 186 [100; Fe(η -C₅H₅)₂]; (ca. 450 °C) 618 [70; H(fcS)₂Fc⁺], 434 [22; FcSfcSH⁺], 402 [70; Fc₂S⁺], 218 [76; FcSH⁺], 186 [100; Fe(η -C₅H₅)₂⁺].

For 9: IR (cm⁻¹) 3088 (vw), 1408 (w), 1382 (w), 1348 (w), 1149 (w), 1017 (m), 875 (w), 819 (m), 483 (m); pyrolysis MS [fc = Fe(η -C₅H₄)₂, Fc = Fe(η -C₅H₅)(η -C₅H₄)] (EI, 70 eV) *m/z* [%] (ca. 350 °C) 790 [0.5; (fcSe)₃⁺], 712 [49; H(fcSe)₂Fc⁺], 528 [10; (fcSe)₂⁺], 450 [100; H(fcSe)Fc⁺].

Anionic ROP of 6. To a rapidly stirred solution of **6** (0.075 g, 0.35 mmol) in THF (2 mL) was added n-BuLi (0.014 mmol, 1:25 ratio). After 1 h, the red solution became cloudy. The reaction mixture was stirred at room temperature for 3 d, after which it changed to an orange color with the formation of an orange precipitate. The reaction was quenched by the addition of three drops of water, and the THF-insoluble material was collected to give **8** as an orange, insoluble solid in a yield of 0.011 g (14%).

Anionic Oligomerization of 6. With stirring, a suspension of fC₅H₄·TMEDA (0.070 g, 0.22 mmol) in THF (3 mL) was added to **6** (0.050 g, 0.23 mmol). Over a period of several minutes, a color change was noted from red to orange with the formation of a small amount of a light-colored precipitate. After 5 min of stirring, Me₃SiCl (100 μ L, 0.79 mmol) was added to the reaction mixture. The solvent and excess Me₃SiCl were removed *in vacuo*, and the product was extracted with hexanes (3 \times 10 mL). After filtration, the solvent was removed *in vacuo* and the residue was column chromatographed on alumina (85:15 cyclohexanes/CH₂Cl₂). Three bands were isolated and collected. The first band was identified as Fe(C₅H₄SiMe₃)₂ by TLC comparison with an authentic sample. After solvents were removed *in vacuo* and the residue was recrystallized from hexanes, amber crystalline **10b** and **11b** were isolated from the second and third band, respectively.

For 10b: yield = 20 mg (16%); *R_f* (15:85 CH₂Cl₂/cyclohexane) 0.27; ¹H NMR (C₆D₆) δ (ppm) 4.31 (m, 8H, Cp), 4.06 (t, *J* = 2 Hz, 4H, Cp), 3.92 (t, *J* = 2 Hz, 4H, Cp), 0.26 (s, 18H, Me); ¹³C NMR (C₆D₆) δ (ppm) 83.8 (*ipso*-Cp-S), 74.7 (Cp-H), 73.3 (*ipso*-Cp-SiMe₃), 73.1 (Cp-H), 73.0 (Cp-H), 69.2 (Cp-H), 0.1 (Si(CH₃)₃); MS (EI, 70 eV) *m/z* [%] 546 [100; M⁺], 73 [24; SiMe₃].

For 11b: yield = 10 mg (7%); *R_f* (15:85 CH₂Cl₂/cyclohexane) 0.10; ¹H NMR (C₆D₆) δ (ppm) 4.32 (m, 12H, Cp), 4.06 (t, *J* = 2 Hz, 4H, Cp), 4.01 (t, *J* = 2 Hz, 4H, Cp), 3.93 (t, *J* = 2 Hz, 4H, Cp), 0.26 (s, 18H, Me); MS (EI, 70 eV) *m/z* [%] 762 [100; M⁺].

Synthesis of Fe(η -C₅H₃Me)₂S (12**).** Butyllithium in hexanes (20.2 mL, 1.49 M, 30.1 mmol) was added to a solution of dimethylferrocene (3.23 g, 15.1 mmol) in hexanes (ca. 150 mL) and TMEDA (2.7 mL, 18 mmol). After 3 d of stirring, the deep red solution was evaporated to dryness *in vacuo* leaving a red gummy material.

The dilithiodimethylferrocene was dissolved in diethyl ether (ca. 50 mL), and the resulting solution was slowly added to a frozen suspension of S(O₂SPh)₂ (5.74 g, 18.2 mmol) in ether (ca. 50 mL) at -196 °C. This was slowly allowed to warm to -78 °C in a dry ice/acetone bath. The orange-red reaction mixture was kept at this temperature for 3 h, after which it turned a deep red color. Hexanes (100 mL) was added to the red solution, and the resulting solution was filtered (-78 °C) through a 3 cm bed of alumina which was then washed repeatedly with hexanes (ca. 200 mL) until only a light pink color was observed in the filtrate. The resulting filtrate was collected, and the solvent was removed *in vacuo* to give a red-purple oil. This oil was redissolved in

hexanes (ca. 50 mL), and the resulting solution was filtered again through a 3 cm plug of alumina which was subsequently washed with hexanes. After the solvent was removed *in vacuo*, **12** was isolated as a purple oil in a yield of 1.23 g (33%).

For **12**: ^1H NMR (C_6D_6) δ (ppm) 4.5–4.7 (mult., Cp) and 3.7–4.1 (m, Cp) (total, 6H), 1.5–2.2 (mult., Me, 6H); ^{13}C NMR (C_6D_6) δ (ppm) 93.1, 92.3, 91.8 (*ipso*-Cp-Me), numerous peaks in the region 89.0–68.2 (Cp-H), 14.9, 14.8, 14.5, 14.0, 13.7 (Me), 12.7, 11.6 (*ipso*-Cp-S).

Compound **12** (0.35 g) was dissolved in hexanes (ca. 4 mL) and cooled at -40 °C overnight, resulting in the precipitation of the enantiomer mixture **12a** in a yield of 0.05 g.

For **12a**: ^1H NMR (200 MHz, C_6D_6) δ (ppm) 4.63 (dd, $J = 1.2$ Hz, 2H), 4.53 (t, $J = 1.5$ Hz, 2H), 3.88 (t, $J = 1.9$ Hz, 2H), 1.65 (s, 6H); ^{13}C NMR (75.4 MHz, C_6D_6) δ (ppm) 93.2 (*ipso*-Cp-Me), 82.2 (Cp-H), 81.6 (Cp-H), 78.2 (Cp-H), 14.8 (Me), 11.7 (*ipso*-Cp-S); MS (EI, 70 eV) m/z [%] 244 [38; M^+], 188 [100; $\text{M}^+ - \text{Fe}$], 156 [54; $\text{M}^+ - \text{FeS}$].

Thermal ROP of 12. A Pyrex tube was charged with **12** (20 mg) and heated to 160 °C in an oil bath under nitrogen. An immediate reaction was observed, and a brown cloud of smoke was formed in the tube. The heat source was removed, and the smoke was then removed *in vacuo*. The remaining brown solid was extracted with 3 mL of toluene and subsequently filtered and precipitated into methanol. After drying, 10 mg (50%) of beige poly(ferrocenyl sulfide) **13** was isolated. This material was found to be soluble in toluene and THF, but not in CH_2Cl_2 .

For **13**: ^1H NMR (300 MHz, C_6D_6) δ (ppm) 4.2 (br, Cp) and 4.0 (br, Cp) (total, 6H), 2.2 (br, Me) and 1.8 (br, Me) (total, 6H); ^{13}C NMR (75.4 MHz, C_6D_6) δ (ppm) 75.5, 74.5, 73.3, 72.0, 69.1, 67.8 (Cp), 14.0, 12.8 (Me); GPC (THF vs polystyrene) $M_w = 11\,500$, $M_n = 5900$; CV (0.1 M $[\text{Bu}_4\text{N}][\text{PF}_6]$ in THF) $\Delta E = 0.33$ V.

Alternatively, heating a solution of **12** (0.41 g, 1.7 mmol) in xylenes (ca. 2 mL) in a sealed evacuated Pyrex tube at 140 °C for 2 h resulted in the formation of a dark-brown solution containing an insoluble solid. After the solution was cooled, the mixture was filtered and precipitated into methanol (200 mL). The dark beige-orange solid was then redissolved in a minimum amount of THF (ca. 2 mL) and reprecipitated into methanol (200 mL) to give **13** in a yield of 0.064 g (16%).

For **13**: ^1H NMR and ^{13}C NMR spectra of the product are identical to those of the melt-derived product; GPC $M_w = \text{ca. } 9000$; $M_n = \text{ca.}$

3500; IR (cm^{-1}) 3075 (w) 2965 (w), 2946 (w), 2917 (m), 2885 (w), 2865 (w), 1471 (w), 1453 (m), 1373 (m), 1031 (s), 895 (w), 824 (s), 494 (s); UV/vis (THF) λ_{max} (ϵ) 430 nm (390 $\text{L mol}^{-1} \text{cm}^{-1}$); CV (0.1 M $[\text{Bu}_4\text{N}][\text{PF}_6]$ in THF) $E_{1/2}^1 = -0.07$ V, $E_{1/2}^2 = 0.24$ V, $\Delta E = 0.31$ V. Anal. Calcd for $[\text{C}_{12}\text{H}_{12}\text{FeS}]_n$: C, 59.04; H, 4.95. Found: C, 59.64; H, 4.91.

Anionic ROP of 12. A sample of **12** was purified by column chromatography on alumina to remove Me_2fc . To a vigorously stirred solution of **12** (0.62 g, 2.5 mmol) in THF (ca. 10 mL) was added 3.2 μL of butyllithium (1.6 M) (5.1 μmol) by microliter syringe. This was stirred for 2 d, over which time the solution was observed to turn deep amber, and the reaction was quenched by precipitation into MeOH (yield = 0.17 g (27%)). The beige solid formed was analyzed by ^1H NMR and was found to be consistent with the formation of **13**. For **13**: GPC $M_w = \text{ca. } 4300$, $M_n = \text{ca. } 3500$; CV (0.1 M $[\text{Bu}_4\text{N}][\text{PF}_6]$ in THF) $E_{1/2}^1 = -0.09$ V, $E_{1/2}^2 = 0.22$ V, $\Delta E = 0.31$ V.

Acknowledgment. This work was funded by the donors of the Petroleum Research Fund, administered by the American Chemical Society, and the Natural Science and Engineering Research Council of Canada (NSERC). We thank Dr. Dan Foucher (Xerox Research Centre of Canada) for help in obtaining the DSC analyses. D.G. also thanks NSERC for a Graduate Fellowship (1993–97), R.R. thanks the Government of Ontario for an Ontario Graduate Scholarship (1995–96), D.B. thanks Ontario Centre for Materials Research for a Graduate Fellowship (1996–97), and I.M. is grateful to the Alfred P. Sloan Foundation for a Research Fellowship (1994–98), NSERC for an E.W.R. Steacie Fellowship (1997–1998), and the University of Toronto for a McLean Fellowship (1997).

Supporting Information Available: Tables of bond distances, bond angles, atomic coordinates, and thermal parameters for **6**, **7**, **11b**, and **12a**; and full details of EHMO calculations including orbital overlap diagrams (22 pages). See any current masthead page for ordering and Internet access instructions.

JA972043U